Supplemental Materials

Molecular Biology of the Cell

Jonasson et al.

Behaviors of individual microtubules and microtubule populations relative to critical concentrations: Dynamic instability occurs when critical concentrations are driven apart by nucleotide hydrolysis

SUPPLEMENTAL MATERIAL

Table of Contents

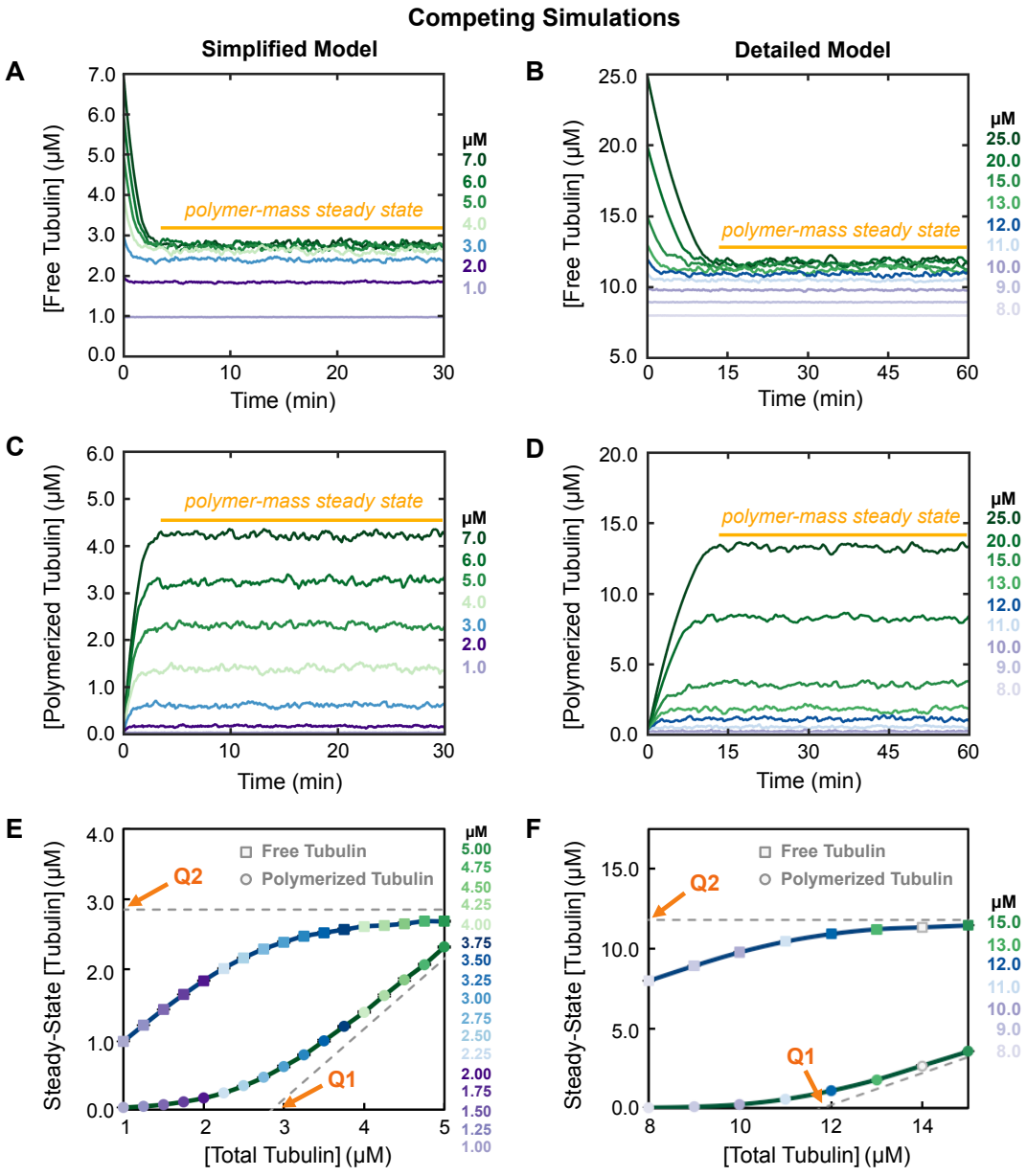

Figure S1: Additional data relevant to Figure 3: the behavior of competing systems of MTs (i.e., systems where [*total* tubulin] is constant). Left panels: simplified model; right panels: detailed model. Colors reflect the concentrations of *total* tubulin (see color keys). ***(A-D)*** The emergent [free tubulin] (panels ***A-B***) and [polymerized tubulin] (panels ***C-D***) as functions of time from one of the three replicates of the simulation runs used in **Figure 3A-B**. ***Interpretation of panels A-D*:** Polymer-mass steady state (as shown by the horizontal line) is when [free tubulin] and [polymerized tubulin] have reached values that stay approximately constant over time. Although there are small fluctuations around the steady-state values, there is no longer a net change over sufficient time. ***(E,F)*** Magnified regions of **Figure 3A-B**. ***Interpretation of panels E,F*:** Detectable polymer exists at [total tubulin] below **Q1** for both the simplified and detailed models. Note that it can be hard to estimate the position of either **Q1** or **Q2** from the magnified region of the datasets shown here. The positions of **Q1** and **Q2** indicated here are from the full datasets shown in **Figure 3A-B**. ***Methods***: Data points in panels **E-F** represent the mean +/- one standard deviation of the values obtained in three independent runs of the simulations.

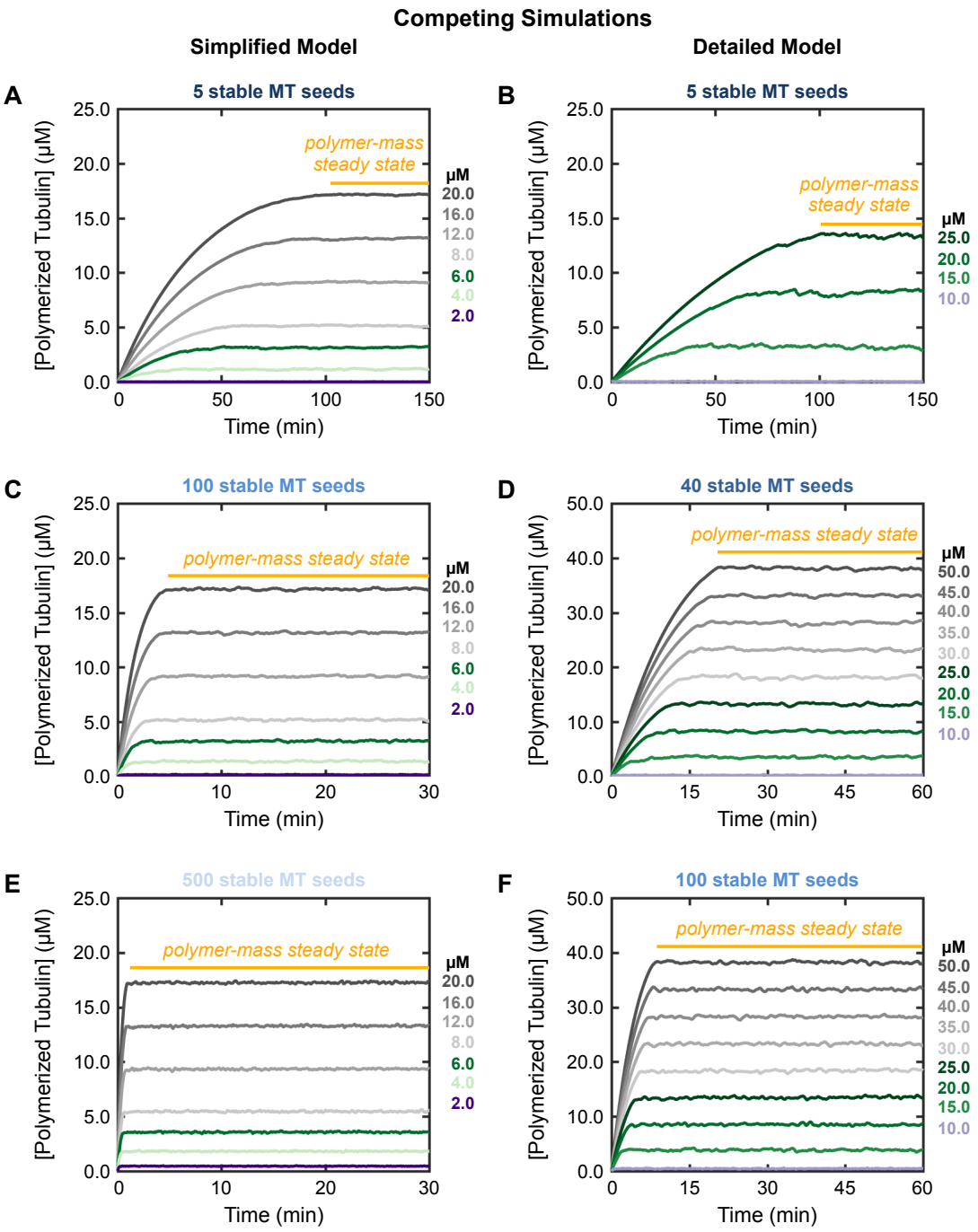

Figure S2: Additional data relevant to Figure 4: varying the number of stable MT seeds in competing systems of MTs. Left panels: simplified model; right panels: detailed model. Colors reflect the concentrations of *total* tubulin (see color keys). **(*A*-*F*)** [Polymerized tubulin] versus time, analogous to **Figure S1C-D**. Simplified model: 5 seeds (panel **A**), 100 seeds (panel **C**; data for [total tubulin] ≤ 6 μM are re-plotted from **Figure S1C**), 500 seeds (panel **E**). Detailed model: 5 seeds (panel **B**), 40 seeds (panel **D**; data for [total tubulin] ≤ 25 μM are re-plotted from **Figure S1D**), 100 seeds (panel **F**). Each plot is from one of the three replicates of the simulation runs used in **Figure 4**. ***Interpretation*:** In both models, the time to reach polymer-mass steady state is longer when there are fewer seeds or when [total tubulin] is higher.

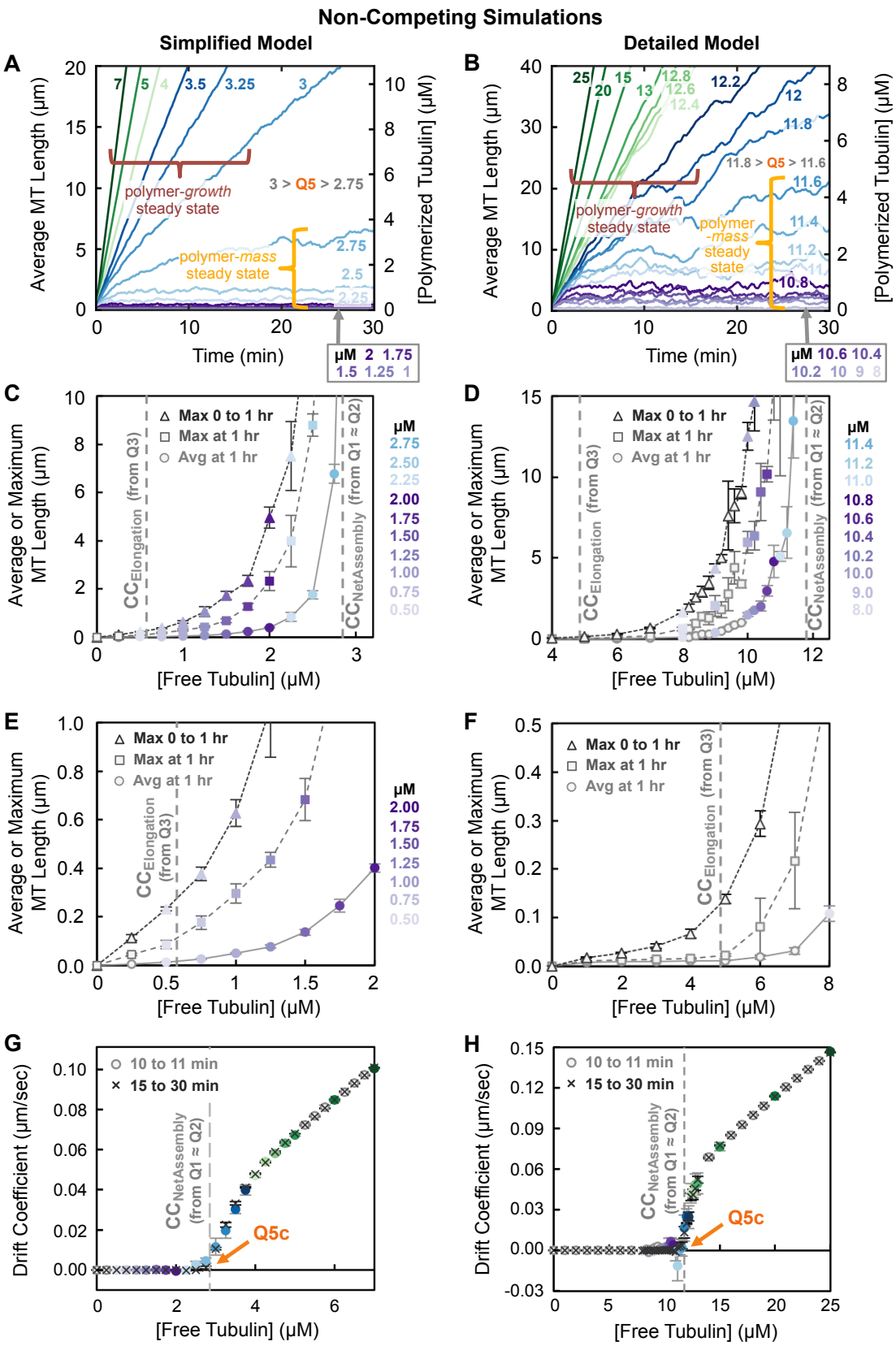

Figure S3 ***(legend on next page)***

Figure S3: Additional data relevant to Figure 5: the behavior of non-competing systems of MTs (i.e., systems where [*free* tubulin] is constant). Left panels: simplified model; right panels: detailed model. Colors reflect the concentrations of *free* tubulin. ***(A,B)*** Average MT length (left axes) and [polymerized tubulin] (right axes) as functions of time from one of the three replicates of the simulation runs used in **Figure 5C-F**. ***Interpretation of panels A,B*:** At [free tubulin] below $CC_{NetAssembly}$ as measured by **Q5**, the system reaches polymer-mass steady state, where the average MT length or [polymerized tubulin] have plateaued. In contrast, at [free tubulin] above $CC_{NetAssembly}$ (**Q5**), there is no polymer-mass steady state, but instead a polymer-growth steady state, where average MT length or [polymerized tubulin] increase at constant rates over time. ***(C-F)*** Average MT length of the population at 1 hour (circles); maximum MT length of the population either at 1 hour (squares) or between 0 to 1 hour (triangles). Panels **E-F** show zoom-ins of the data plotted in panels **C-D**. ***Methods for panels C-F*:** The length here is the length above the seed and the measurements include all 100 stable MT seeds in the simplified model and all 40 stable MT seed in the detailed model, so each empty seed contributes a value of 0 to the average. Data points represent the mean +/- one standard deviation of the values obtained in three independent runs of the simulations. ***(G,H)*** Examination of the effect of changing the total observation time when calculating the steady-state drift coefficient using the time-step analysis method (see Supplemental Methods). The plots show a comparison of the drift coefficients for MT populations observed over a 1-minute interval (o symbol) or over a 15-minute interval (x symbols, re-plotted from **Figure 5E-F**) as functions of [free tubulin]. ***Interpretation of panels G,H*:** These data show that varying the total observation time has an impact on the noise (drift coefficients measured over the 15-minute interval show less noise, as seen by smaller error bars, than those from the 1-minute interval), but the values themselves are not otherwise affected. ***Methods for panels G,H*:** To determine the *steady-state* value of the drift coefficient, the measurements should be performed after the system has reached the appropriate steady state (polymer-mass steady state for [free tubulin] below $CC_{NetAssembly}$, and polymer-growth steady state for [free tubulin] above $CC_{NetAssembly}$). Data points represent the mean +/- one standard deviation of the values obtained in three independent runs of the simulations.

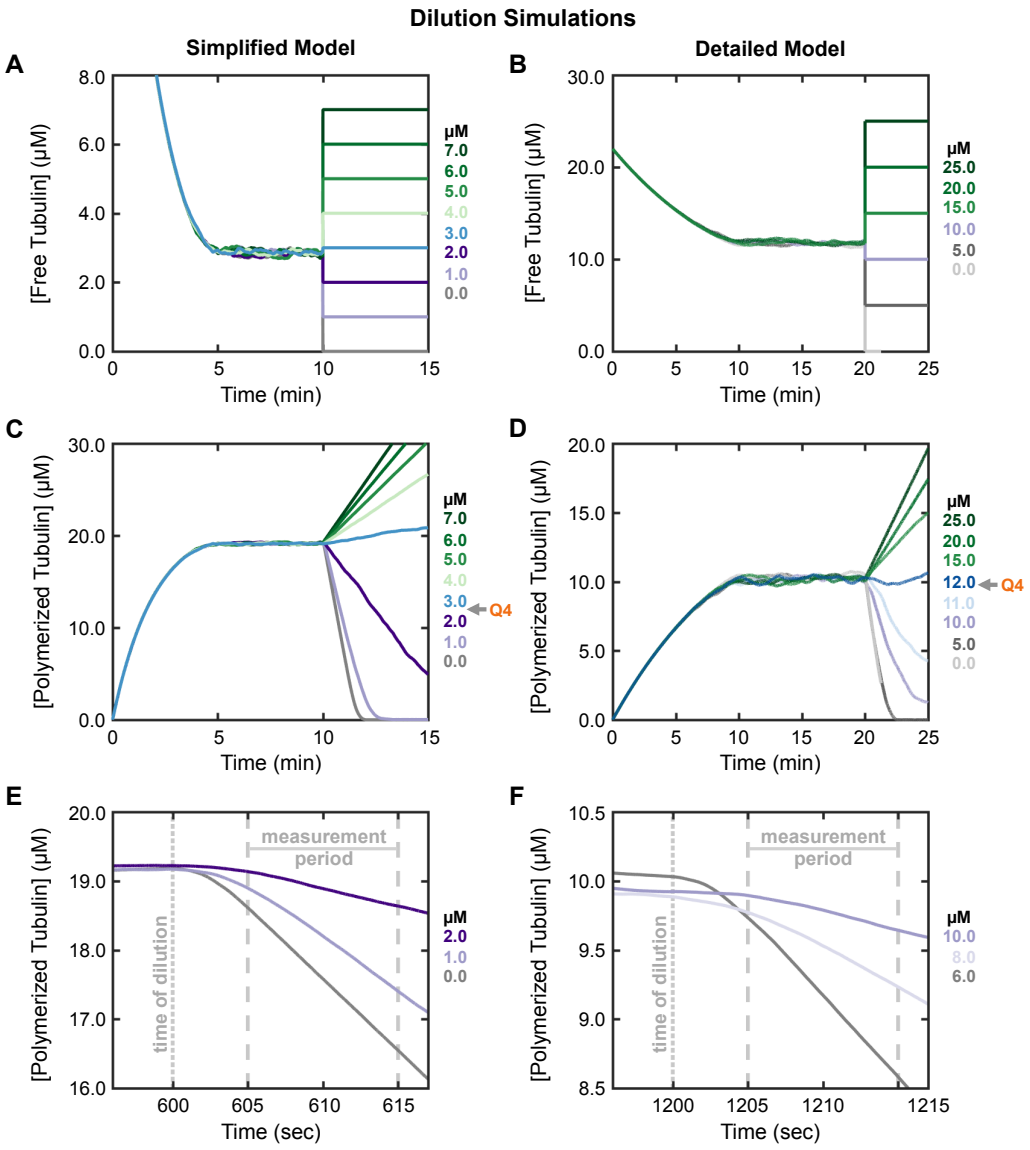

Figure S4: Additional data relevant to Figure 6: measuring the rate of change in [polymerized tubulin], i.e., flux of tubulin into and out of polymer, in the dilution simulations. Left panels: simplified model; right panels: detailed model. Colors reflect the *dilution [free tubulin]*, i.e., the concentration of free tubulin after the dilution. **(*A*-*D*)** Plots of [free tubulin] (panels **A**-**B**) and [polymerized tubulin] (panels **C**-**D**) versus time for selected values of dilution [free tubulin]. **(*E*,*F*)** Plots of [polymerized tubulin] versus time for selected values of dilution [free tubulin] during a time period from shortly before the dilution through the flux measurement period from **Figure 6** (605 to 615 seconds in the simplified model; 1205 to 1215 seconds in the detailed model). ***Interpretation***: At the time of the dilution, the emergent [free tubulin] is approximately equal to $CC_{NetAssembly}$ (panels **A**-**B**). For the dilutions into [free tubulin] above $CC_{NetAssembly}$, the polymer mass increases with time after the dilution; for the dilutions into [free tubulin] below $CC_{NetAssembly}$, the polymer mass decreases with time after the dilution (panels **C**-**D**). As seen in panels **E**-**F**, the delay after the dilution allows the rate of change in [polymerized tubulin] to reach its steady-state value (as expected because the GTP-cap size needs time to respond to the new [free tubulin] (Duellberg et al., 2016; Bowne-Anderson et al., 2013; Mauro et al., 2019). If the measurements were performed without the delay, then the magnitude of the initial rates would be underestimated.

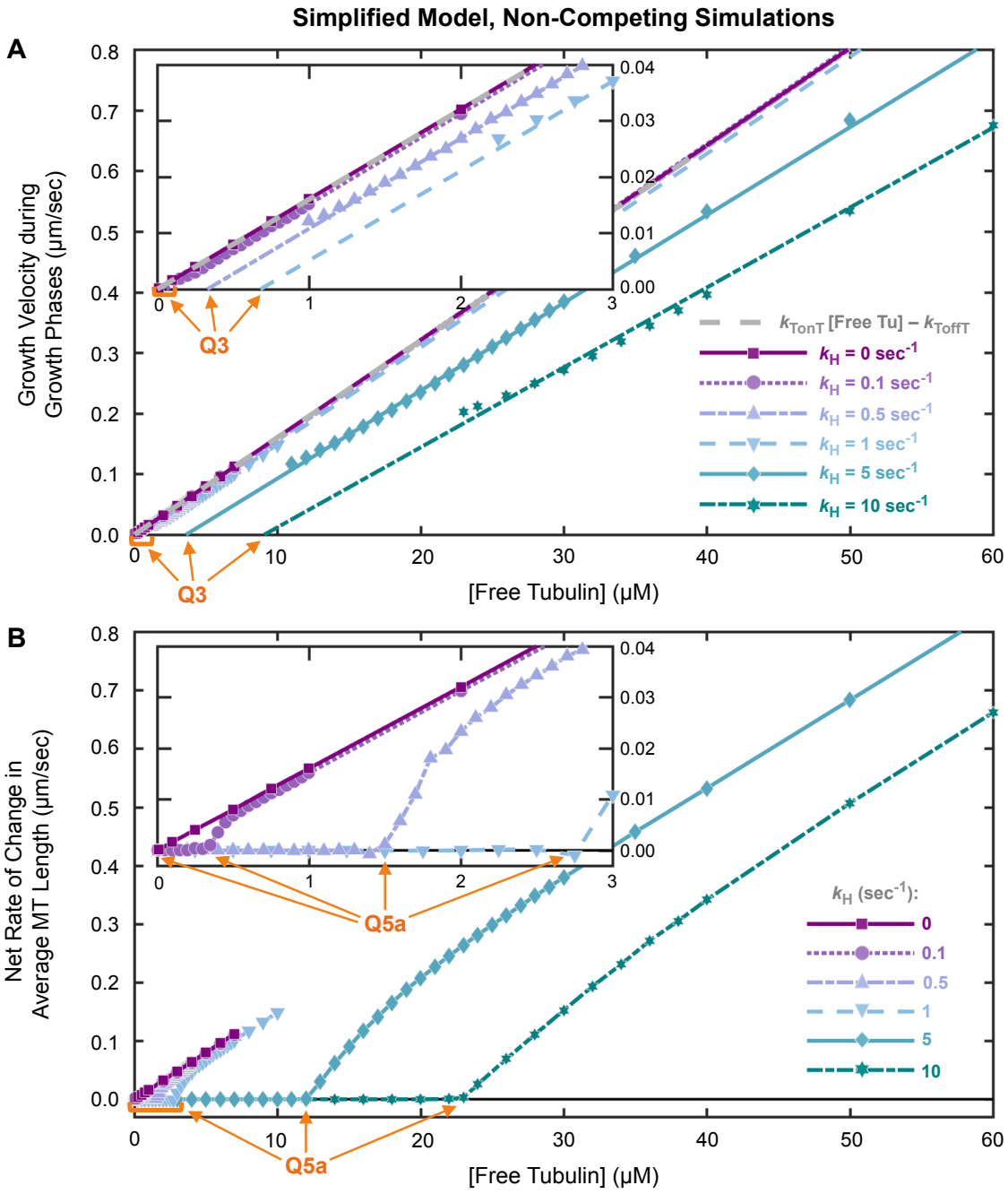

Figure S5: Additional plots relevant to Figure 9: analysis of varying the rate constant for nucleotide hydrolysis (k_H) in the simplified model (non-competing simulations). For comparison across the varying values of k_H, V_g from each of **panels 9A-F** is re-plotted here in panel **S5A**, and $J_{Constant}$ from each of **panels 9A-F** is re-plotted here in panel **S5B**. The insets show zoom-ins at low [free tubulin]. See keys in panels **S5A** and **S5B** for the values of k_H. ***Interpretation*:** $CC_{Elongation}$ as measured by Q3 (panel **A**) and $CC_{NetAssembly}$ as measured by Q5a (panel **B**) each increase as k_H is increased. ***Methods:*** The regression lines in panel **A** (re-plotted here from **Figure 9**) were fitted in the [free tubulin] range from $CC_{NetAssembly}$ to the highest [free tubulin] shown in the **Figure 9** panel for each k_H value. The V_g data points re-plotted here are shown only in the [free tubulin] range were V_g is approximately linear as a function of [free tubulin]; for some of the k_H values, this is a wider range than the range used for fitting the regression line.

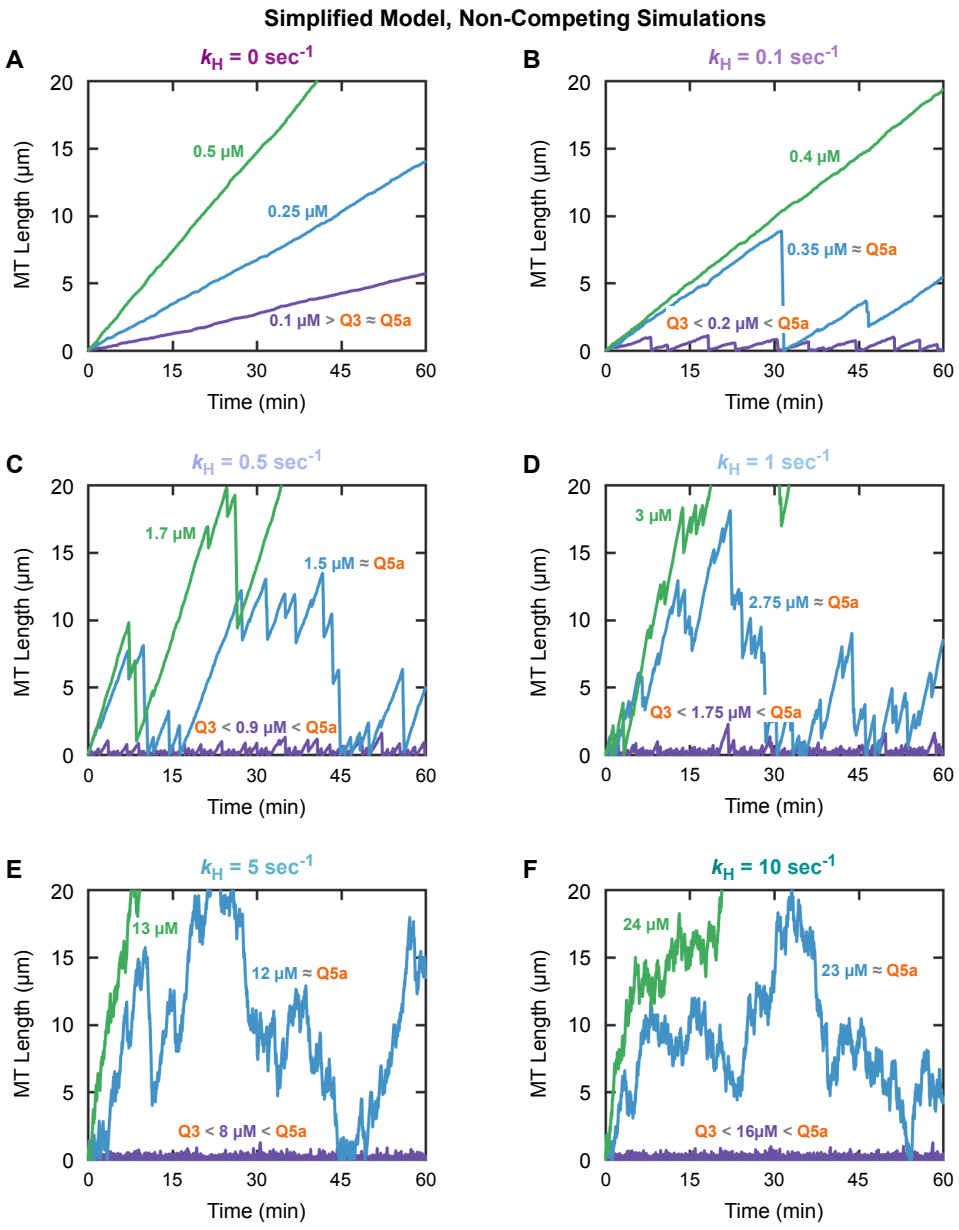

Figure S6: Additional data relevant to Figure 9: individual MT length histories from the simplified model with varying values of the rate constant for nucleotide hydrolysis (k_H). Each of panels **A-F** corresponds to a different value of k_H (see panel titles). ***(A)*** For k_H = 0, length histories are plotted for individual MTs at three different values of [free tubulin] above the CC ($CC_{Elongation}$ = $CC_{NetAssembly}$ when k_H = 0). ***(B-F)*** For each value of k_H > 0, lengths histories are plotted for individual MTs at three different values of [free tubulin]: approximately halfway between $CC_{Elongation}$ and $CC_{NetAssembly}$ (purple); near $CC_{NetAssembly}$ (blue); and slightly above $CC_{NetAssembly}$ (green). ***Interpretation*:** In panel **A**, where k_H = 0 (equilibrium polymer), no dynamic instability (DI) is observed. In panels **B-F**, when k_H > 0 (steady-state polymer), the filaments exhibit DI. Note that for low values of k_H (e.g., panel **B**), DI occurs only within a narrow range of [free tubulin]. As k_H increases, DI occurs over a wider range of [free tubulin] and is therefore more likely to be observed in experiments. For very high k_H (e.g., panels **E-F**), the MTs transition frequently between growth and shortening in contrast to the DI with clearer periods of extended growth and shortening observed at lower k_H.

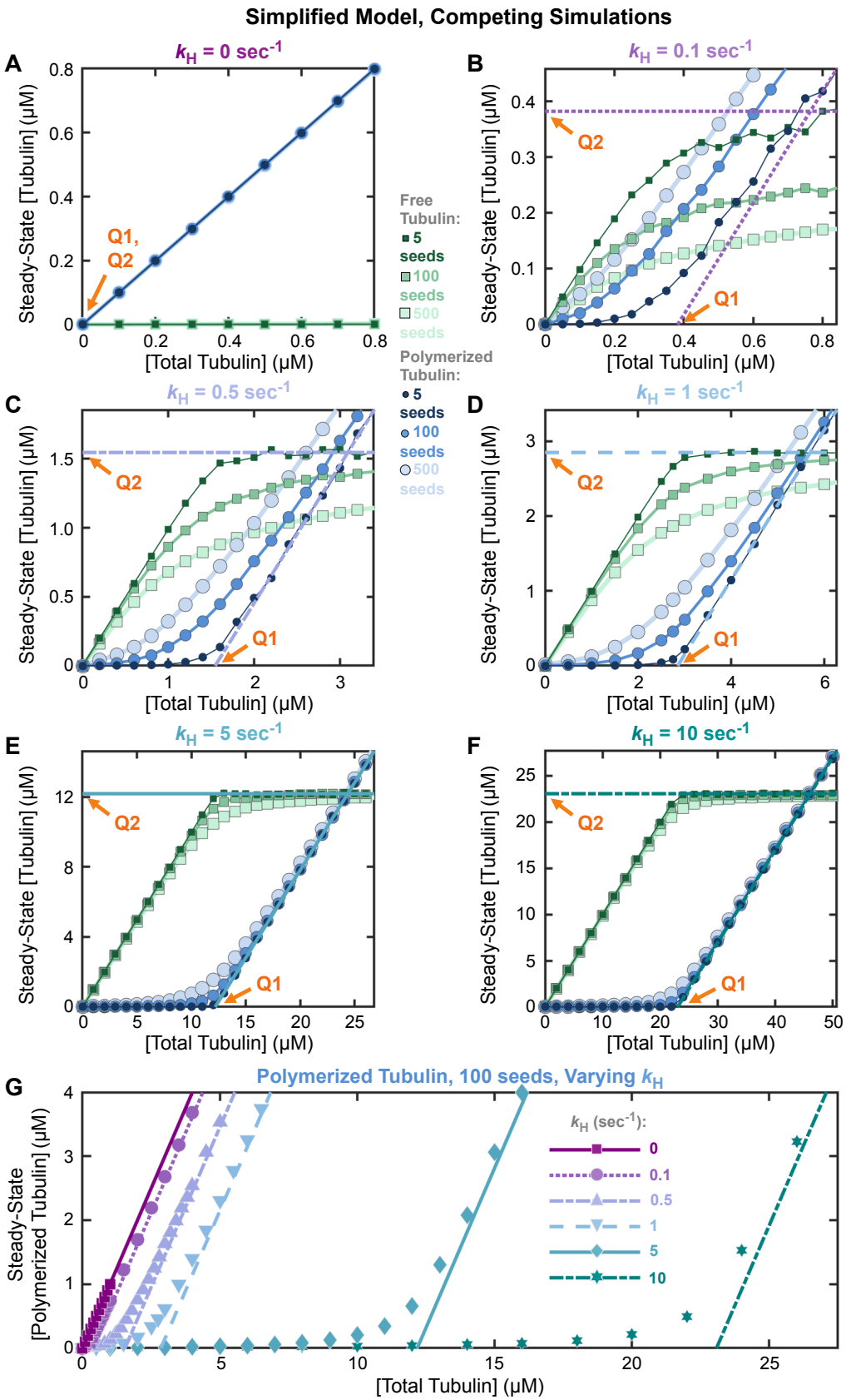

Figure S7 ***(legend on next page)***

Figure S7: Competing simulations with varying k_H in the simplified model. Each of panels **A-F** corresponds to a different value of k_H (see panel titles). **(*A-F*)** [Free tubulin] (green square symbols) and [polymerized tubulin] (blue circle symbols) versus [total tubulin], with 5 seeds, 100 seeds, and 500 seeds, analogous to **Figure 4**. The darker curves with smaller symbols correspond to fewer seeds and the lighter curves with larger symbols correspond to more seeds. Note that the scales of the axes vary among the panels. **(*G*)** For comparison at the same scale, the [polymerized tubulin] versus [total tubulin] curve for each value of k_H with 100 seeds is re-plotted from the corresponding panel from **A-F**. ***Interpretation*:** For each value of k_H, the values of Q1 and Q2 are similar to the value of $CC_{NetAssembly}$ as measured by Q5a (**Figure 9**). As in **Figure 4**, the sharpness of the transition at Q1 and Q2 depends on the number of seeds, and increasing the number seeds leads to a more gradual transition. Panel **G** shows that the gradualness of the transition at Q1 (and therefore also at Q2) increases with increasing k_H. However, panels **B-F** show that when considered relative to $CC_{NetAssembly}$ the gradualness does not necessarily increase with increasing k_H. In other words, the amount of [polymerized tubulin] when [total tubulin] = $CC_{NetAssembly}$ increases with k_H (panel **G**), but the fraction of tubulin that is polymerized (i.e., [polymerized tubulin] divided by [total tubulin]) can decrease with increasing k_H (panels **B-F**). As will be seen by comparing this figure to **Figure S8** (which uses a parameter set with a higher value of CC_{KD_GTP}), it is not the value of k_H itself that determines the sharpness of the transition, but rather the value of k_H relative to the attachment and detachment kinetic rate constants. ***Methods*:** Each data point is from one simulation run with the indicated number of seeds. The simulations for k_H = 1 (panel **D**) correspond to one of the three replicates in **Figure 4**. Similar to **Figures 3** and **4**, [free tubulin] and [polymerized tubulin] from each run were averaged over a period of time after polymer-mass steady state was reached. For k_H = 0 (panel **A**), the averages were taken from 250 to 300 minutes for 5 MT seeds, from 12 to 14 minutes for 100, from 2 to 2.5 minutes for 500 MT seeds. For k_H > 0 (panels **B-G**), the averages were taken from 100 to 300 minutes for 5 MT seeds, and from 15 to 30 minutes for 100 and 500 MT seeds.

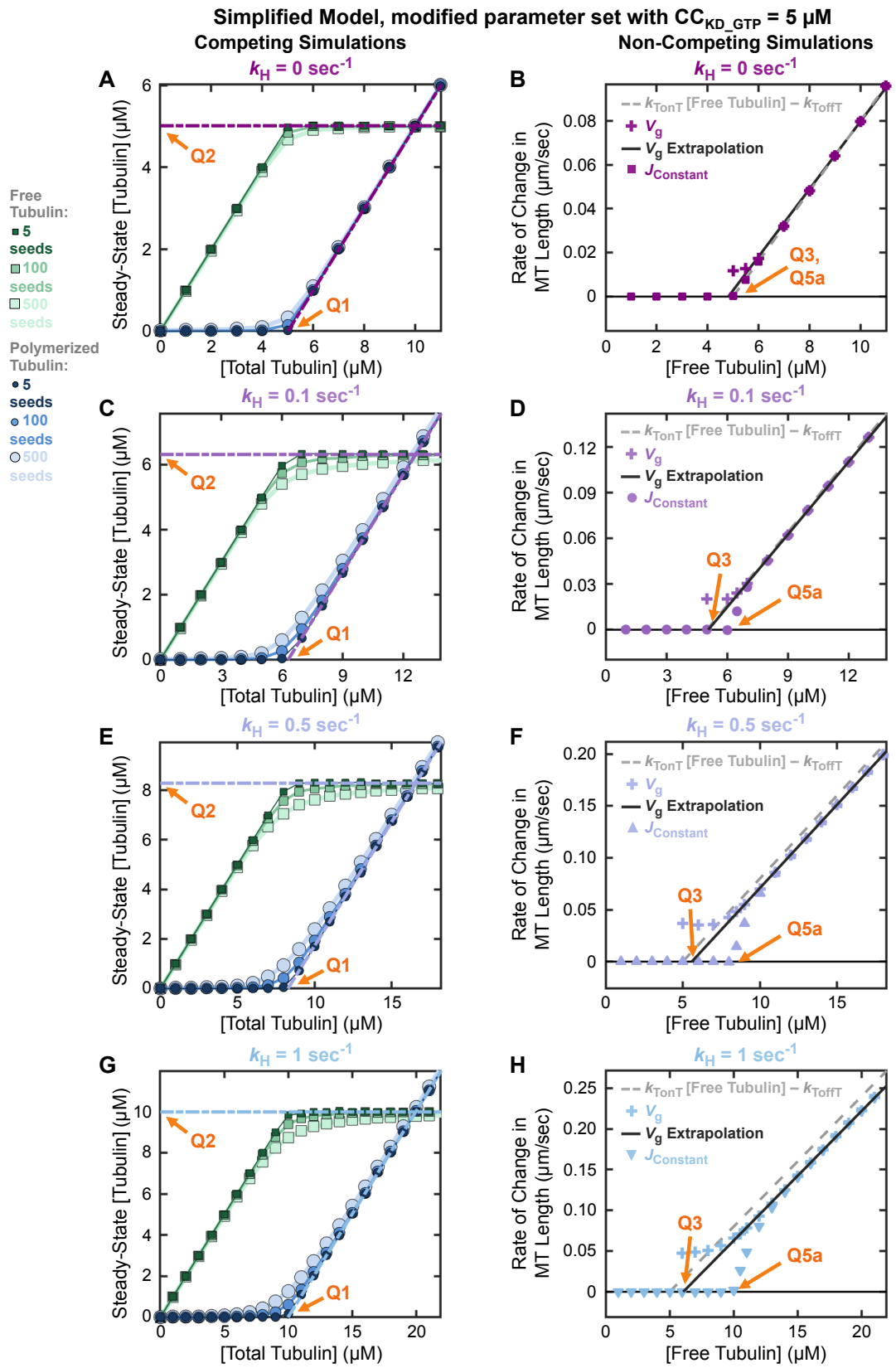

Figure S8 ***(legend on next page)***

Figure S8: Competing and non-competing simulations in the simplified model using a parameter set with CC_{KD_GTP} = 5 µM and varying k_H. In the standard parameter set (see Methods section) used in the simplified model in all other figures, CC_{KD_GTP} = 0 µM. For the simulations in this figure, we increased the kinetic rate constant for detachment of GTP-tubulin to 10 s^{-1}, yielding CC_{KD_GTP} = 5 µM. Left panels: competing simulations; right panels: non-competing simulations. Note that the scales of the axes vary among all panels. **(*A,C,E,G*)** [Free tubulin] (green square symbols) and [polymerized tubulin] (blue circle symbols) versus [total tubulin] from competing simulations with 5 seeds, 100 seeds, and 500 seeds. The darker curves with smaller symbols correspond to fewer seeds and the lighter curves with larger symbols correspond to more seeds. **(*B,D,F,H*)** V_g and $J_{Constant}$ from non-competing simulations. For comparison, we also plot the theoretical equation for V_g that assumes that growing ends have only GTP-tubulin at the tips (grey dashed line). ***Interpretation*:** For each value of k_H, the value of $CC_{NetAssembly}$ as measured by Q1 and Q2 (left column) is consistent with the value as measured by Q5a (right column). As k_H is increased, $CC_{Elongation}$ (Q3) and $CC_{NetAssembly}$ (Q1, Q2, Q5a) both increase and diverge from CC_{KD_GTP} (horizontal intercept of grey dashed lines, right column), consistent with the conclusions drawn for the standard parameter set (**Figures 9, S5-S7**). Similar to **Figure S7**, the gradualness of the transition at Q1 (and Q2) increases with increasing k_H. However, the sharpness of the transition when considered relative to $CC_{NetAssembly}$ is not as gradual for low k_H here as it is in **Figure S7**. Thus, comparison with **Figure S7** shows that it is not the value of k_H itself that determines the sharpness of the transition, but rather the value of k_H relative to the attachment and detachment kinetic rate constants. ***Methods*:** *Competing simulations (left column)*: One simulation run was performed at each [total tubulin] for each of the indicated number of seeds. Similar to **Figures 3**, **4**, and **S7**, [free tubulin] and [polymerized tubulin] from each run were averaged over a period of time after polymer-mass steady state was reached. The averages were taken from 250 to 300 minutes for 5 MT seeds with k_H = 0, from 100 to 300 minutes for 5 MT seeds with k_H > 0, and from 15 to 30 minutes for 100 and 500 MT seeds for all k_H. *Non-competing simulations (right column)*: One simulation run with 50 stable MT seeds was performed at each [free tubulin]. V_g was measured using the DI analysis method (described in Supplemental Methods; same analysis method used to measure V_g in **Figures 7** (+ symbols), **9** (+ symbols), **S5A** (symbols vary by k_H value)). The steady-state rate of change in average MT length, $J_{Constant}$, was measured using the *net* change method (**Table S1B**; see also Q5a, **Table 3B**; same method used to measure $J_{Constant}$ in **Figure 5C-F** (circle symbols), **9** and **S5B** (symbols vary by k_H value)). All V_g and $J_{Constant}$ measurements in this figure were taken from 40 to 60 minutes. V_g data points are plotted only at concentrations where detected growth phases constituted at least 2% of the total time analyzed (20 min * 50 MTs = 1000 min analyzed). Regression lines (black solid lines) were fitted to the V_g data points in the [free tubulin] range above $CC_{NetAssembly}$ and then extrapolated back to V_g = 0.

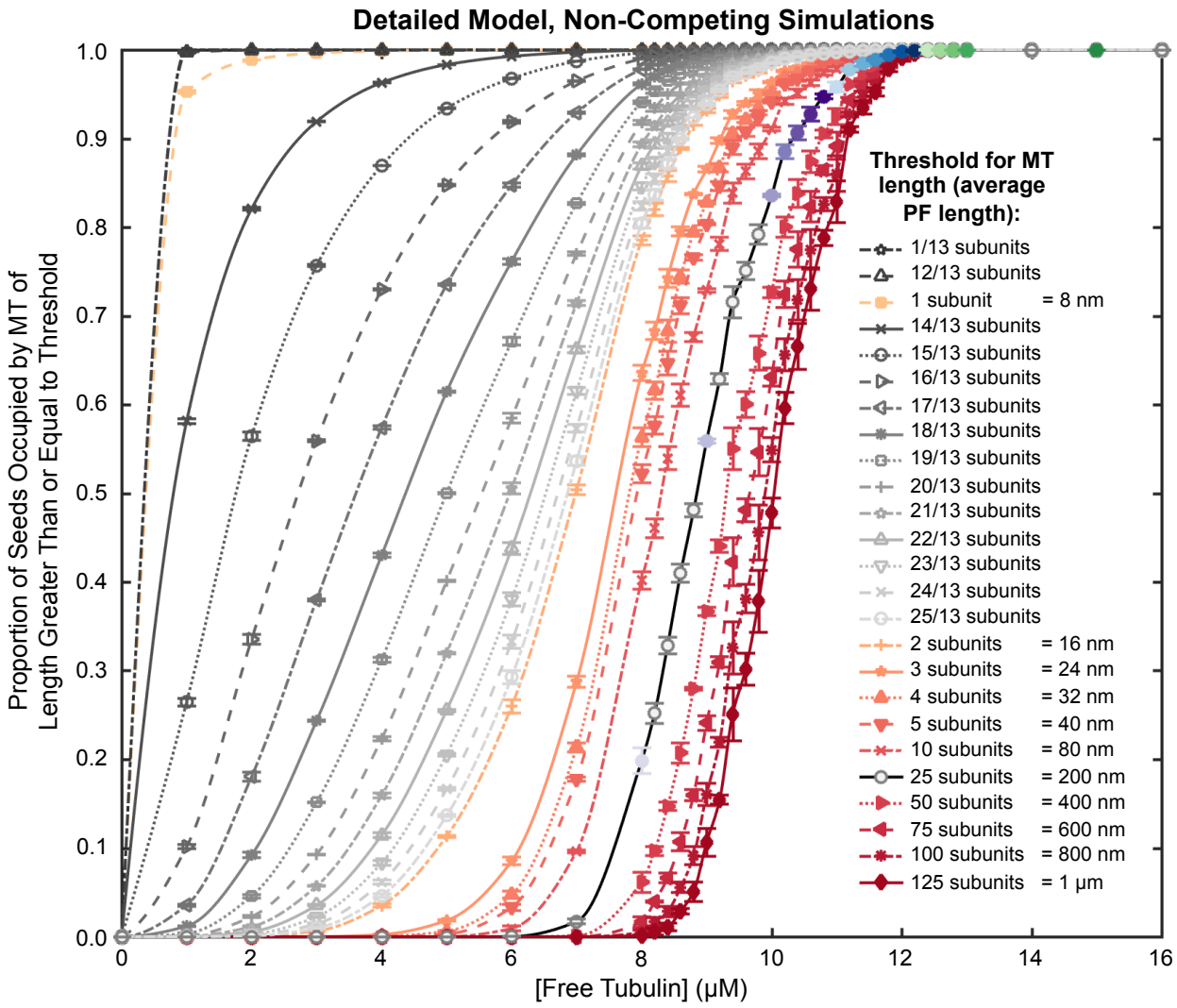

Figure S9: Detailed model P_{occ} (proportion of occupied seeds) with additional thresholds. As in **Figure 10**, P_{occ} is the fraction of the stable seeds bearing a microtubule with length greater than or equal to the given threshold. In the detailed model, the MT length is the average of the 13 protofilament lengths and can therefore have non-integer values. The thresholds with integer values (in units of subunit lengths) are re-plotted from **Figure 10D**. ***Interpretation*:** The fractional thresholds from 14/13 subunits to 25/13 subunits shown here demonstrate how the P_{occ} curve varies as the threshold changes from 1 subunit to 2 subunits. These data show that the sigmoidal shape of the P_{occ} curve emerges and becomes increasingly steep as the detection threshold is increased. ***Methods*:** All data points represent the mean +/- one standard deviation of the values obtained in three independent runs of the simulations with constant [free tubulin]. The values from each run are averages from 25 to 30 minutes.

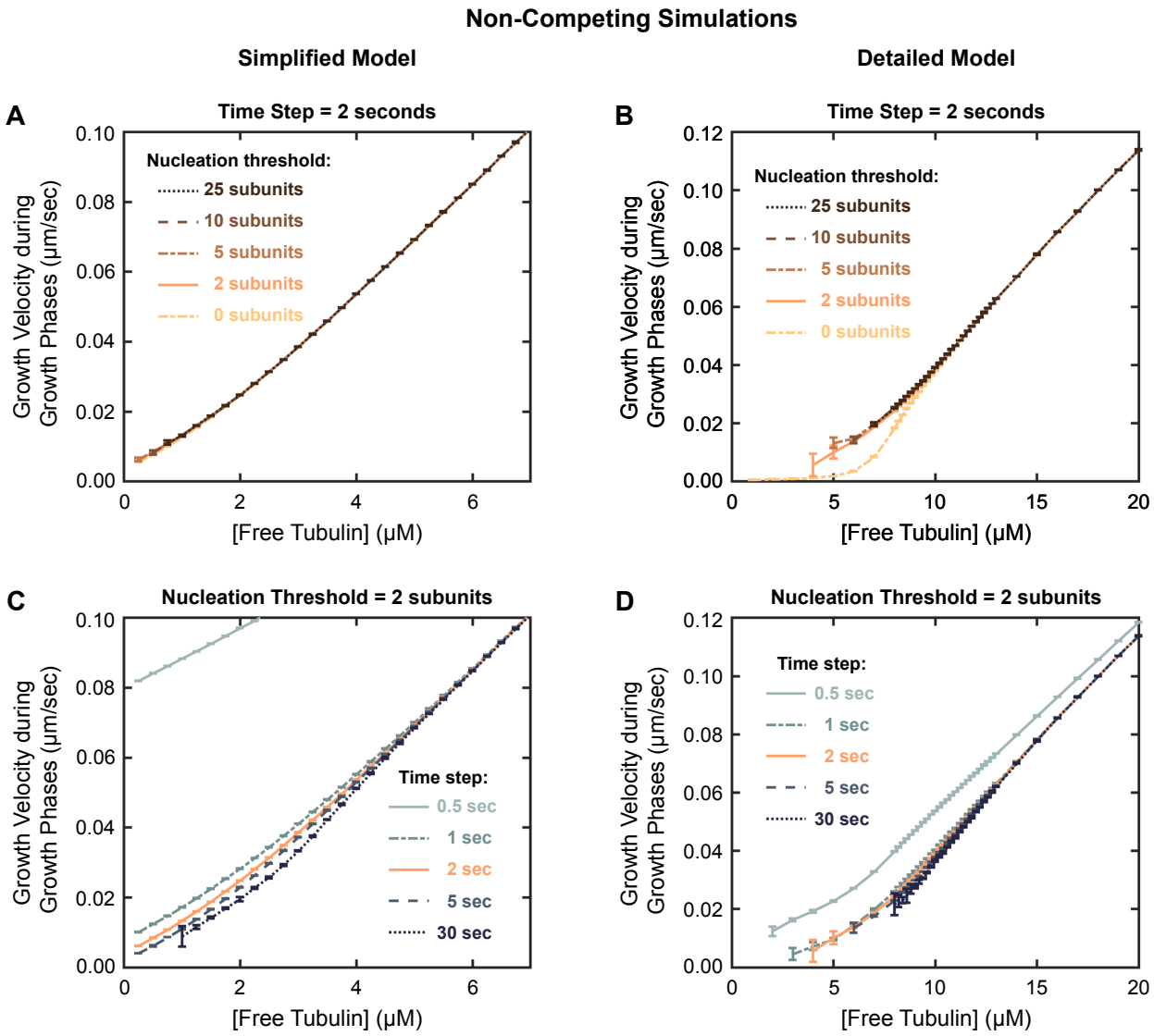

Figure S10: Effect of time-step duration and "nucleation" threshold in the time-step method for measuring growth velocity (V_g) described in the Supplemental Methods. Left panels: simplified model; right panels: detailed model. **(*A,B*)** Time step = 2 seconds, with varying nucleation thresholds (1 subunit length = 8 nm). **(*C,D*)** Nucleation threshold = 2 subunit lengths, with varying time steps. ***Interpretation*:** Based on these results of varying the nucleation threshold and the time step, we chose a time step of 2 seconds and a nucleation threshold of 2 subunit lengths for the analysis in **Figure 7** (square symbols, all panels). In particular, the data in **Figure 7A-B** (square symbols) is the same as the data plotted here for time step = 2 seconds and nucleation threshold = 2 subunit lengths. *Consequences of changing the nucleation threshold*: Using a lower nucleation threshold underestimates V_g, particularly noticeable in the detailed model (panel **B**). Using a higher nucleation threshold increases the minimum concentration at which data are obtained (panels **A-B**). *Consequences of changing the time step*: Using a shorter time step overestimates V_g. Using a longer time step underestimates V_g and increases the minimum concentration at which data are obtained (panels **C-D**). See Supplemental Methods for additional information and interpretations.

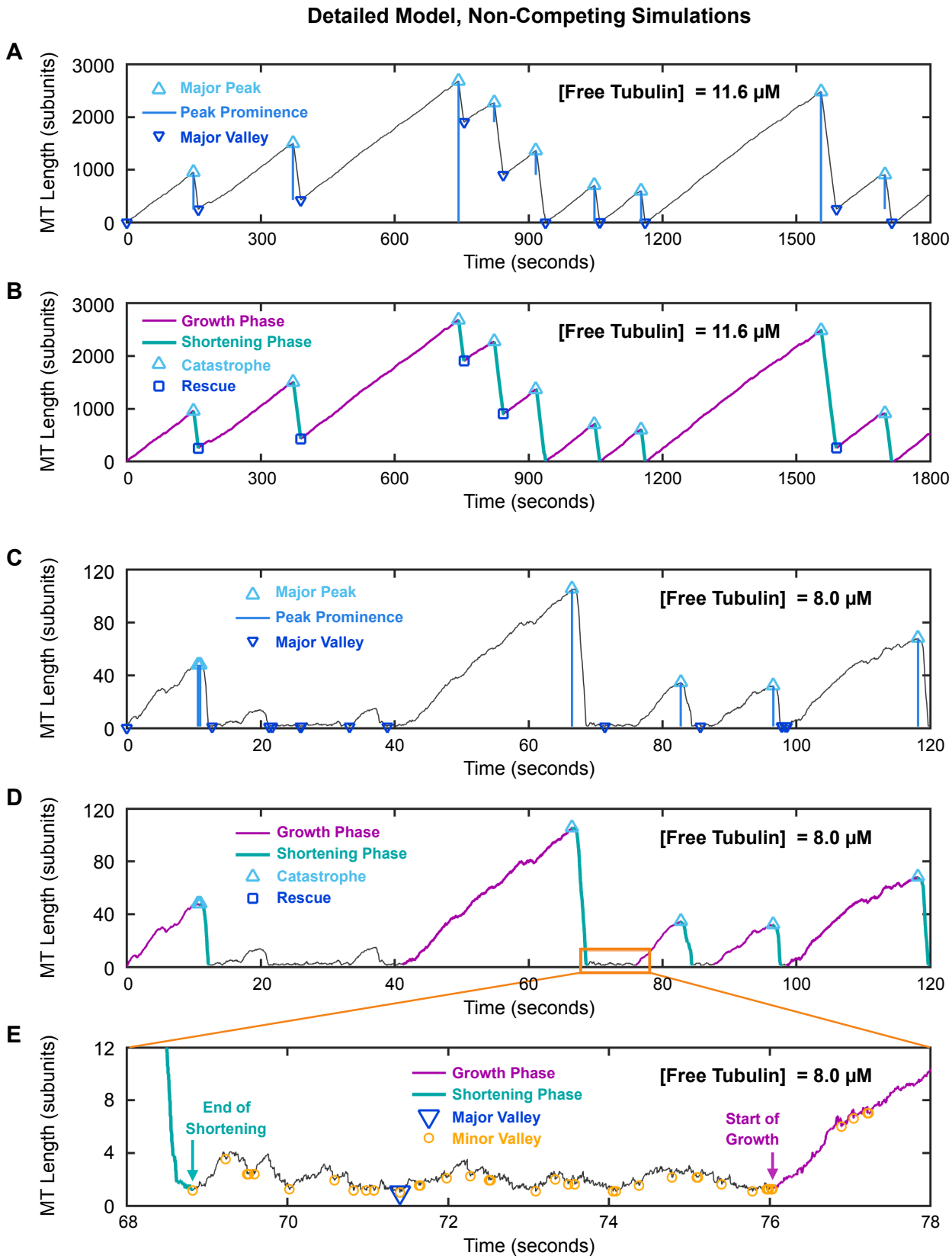

Figure S11 ***(legend on next page)***

Figure S11: Length histories illustrating the DI analysis method described in the Supplemental Methods. Representative length histories from the detailed model under constant [free tubulin] conditions at 11.6 μM (panels **A-B**) and at 8 μM (panels **C-E**), chosen to highlight different aspects of DI. **(*A,C*)** Identification of major peaks and valleys (those with prominence ≥ 25 subunit lengths = 200 nm) in length history data. The peak prominence is the vertical distance between the peak and the valley that is nearest to the peak, without a larger intervening peak (the nearest valley can be either before or after the peak)**. (*B,D*)** Identification of the growth phases, shortening phases, catastrophes, and rescues. The ascent to each major peak is classified as a growth phase (purple), and the descent from each major peak is classified as a shortening phase (teal). Transitions from growth to shortening are called catastrophes (light blue triangles) and occur at major peaks. Transitions from shortening to growth, without depolymerization back to the seed, are called rescues (dark blue squares, panel **B**); we classify major valleys as rescues only if the MT length at the major valley is greater than or equal to the rescue threshold (25 subunit lengths = 200 nm). **(*E*)** Determining the end point of a shortening segment (teal) and the start point of a growth segment (purple) when a major valley occurs below the rescue threshold (25 subunit lengths = 200 nm). The end of a shortening phase is identified as the *first minor* valley that occurs after the MT length has shortened to within 1 subunit length of the first *major* valley after the shortening phase. The start of a growth phase is identified as the *last minor* valley that is within one subunit length of the major valley and before the next peak. **All panels:** The vertical axes show the MT length (average of the 13 protofilament lengths) above the stable MT seed in units of subunit length (1 subunit length = 8 nm).

Table S1A. Flux (*J*) abbreviations.

Abbreviation	*Definition*
J	J = rate of change in [polymerized tubulin] = flux of tubulin into and out of polymer (e.g., in µM/s) or [1] J = rate of change in average MT length = drift coefficient (e.g., in µm/s).
$J_{Constant}$	$J_{Constant}$ is J as measured in a constant [free tubulin] experiment (non-competing experiment). When $J_{Constant}$ has reached its steady-state value, $J_{Constant} = 0$ for constant [free tubulin] < $CC_{NetAssembly}$, and $J_{Constant} > 0$ for constant [free tubulin] > $CC_{NetAssembly}$.
$J_{Dilution}$	$J_{Dilution}$ is J as measured in a dilution experiment. When $J_{Dilution}$ has reached its steady-state value for the dilution [free tubulin], $J_{Dilution} < 0$ for dilution [free tubulin] < $CC_{NetAssembly}$, and $J_{Dilution} > 0$ for dilution [free tubulin] > $CC_{NetAssembly}$.

Table S1B. *J* measurement methods. In this article, we measure $J_{Constant}$ using the three different methods listed here, and we measure $J_{Dilution}$ using the Net Change method (for application of the other two methods to J from dilution simulations, see Mauro et al., 2019).

Measurement Method	*Description*
Net Change (Figure 5C-F, circle symbols)	J is determined from the net change between two time points (called J_{Net} in Mauro et al., 2019): J = ([polymerized tubulin] at time B – [polymerized tubulin] at time A) / (time B – time A) or [1] J = (average MT length at time B – average MT length at time A) / (time B – time A).
J_{DI} Equation (Figure 5C-D, plus symbols)	J is calculated by evaluating the J_{DI} equation with measured values of the DI parameters. See **Equation 1a,b** of the main text. The $J_{DI\_piecewise}$ equation (**Equation 1b**) approximates $J_{Constant}$ (Figure 5C-D). The J_{DI} equation (**Equation 1a**) approximates $J_{Dilution}$ (Figure 10A of Mauro et al., 2019).
Time-Step (Figure 5E-F, x symbols)	J is calculated by summing displacements measured over short time steps based on the drift coefficient method of (Komarova et al., 2002). See **Equation S1** of the Supplemental Methods, called v_d in (Komarova et al., 2002) and called $J_{TimeStep}$ in (Mauro et al, 2019).

[1] The rate of change in [polymerized tubulin] and the rate of change in average MT length can be interconverted as follows:

$$\left(\text{rate of change in [polymerized tubulin] in } \frac{\mu M}{s}\right) = \left(\frac{(\#\text{ of MT seeds}) * (13\text{ protofilaments}) * (125\text{ subunit lengths per } \mu m)}{(\text{volume in fL}) * (\text{Avogadro's number} / 10^{21})}\right) * \left(\text{rate of change in average MT Length in } \frac{\mu m}{s}\right).$$

In the detailed model, the length of each MT is the average of its 13 protofilament lengths. In the simplified model, each subunit represents a 1x13 ring of tubulin dimers. In both models, the average MT length of the population is calculated as an average over all MT seeds in the population, and 1 subunit length = 8 nm.

SUPPLEMENTAL METHODS

Measuring drift coefficient from time-step analysis

The drift coefficient is a measure of the rate of displacement of the MT ends. If one end of a MT is fixed (as in our simulations), then the rate of displacement of the free end is equal to the rate of change in the MT's length. We calculated drift coefficients for our simulation data (**Figures 5E-F**, **S3G-H**) using the drift coefficient formula of (Komarova et al., 2002):

$$v_{\mathrm{d}} = \frac{\sum s_i}{\sum t_i} \qquad \text{(Equation S1)}$$

where v_{d} is the drift coefficient, s_i is the displacement of a MT end, and t_i is the corresponding time between sequential frames in a time-lapse movie. In (Komarova et al., 2002), where this formula was applied to experimental data analyzed by subtraction of image intensities from sequential frames, the time between successive frames was 3 to 5 seconds.

To apply this approach to our simulation data, we calculated the displacements (s_i) of each MT end over time steps (t_i) of 2 seconds. For each [free tubulin] separately, we then summed these displacements of the MT ends ($\sum s_i$) over the population and over time for either 30 time steps (from minute 10 to minute 11 in the simulation; **Figure S3G-H**, o symbols) or 450 time steps (from minute 15 to minute 30 in the simulation; **Figures 5E-F** and **S3G-H**, x symbols). The sum of the displacements over the population and over time ($\sum s_i$) and the sum of the corresponding time changes ($\sum t_i$) were plugged into the above formula for v_d (Equation S1) to obtain the drift coefficient for each free tubulin concentration (**Figures 5E-F**, **S3G-H**). For example, in the simulation data, if 100 MTs are measured over 30 time steps, then $\sum s_i$ and $\sum t_i$ are each the sum of 100*30 = 3000 values. For experimental data, the same number of MTs would not necessarily be observed in every frame, so the sums would just include all displacements that are measured.

When applying the time-step analysis method to experimental data, the displacements that can be detected would depend on the experimental imaging resolution. For our simulated data, we did not impose any detection threshold on the magnitude of displacement (i.e., $|s_i|$) during each time step (see (Mauro et al., 2019) for the effect of imposing such a threshold).

To identify Q5c (**Figures 5E-F**, **S3G-H**), the measurements should be taken during a time period when the drift coefficients have reached their steady-state values (this will occur at polymer-mass steady state for [free tubulin] below Q5 and at polymer-growth steady state for [free tubulin] above Q5). The time-step method described here could also be used to measure drift coefficients at earlier times if one wishes to examine the approach to steady state.

Measuring V_g from time-step analysis

The time-step analysis described above can also be used to obtain measurements of V_g (**Figure 7**, square symbols). To do so, the sums are restricted to include only positive displacements:

$$V_g = \frac{\sum_{pos} s_i}{\sum_{pos} t_i}$$

where $\sum_{pos} s_i$ is the sum of all displacements satisfying $s_i > 0$, and $\sum_{pos} t_i$ is the sum of the corresponding time changes. (When applying this method to experiments with physical detection limits, the sum would include only displacements satisfying $s_i \geq$ the detection limit for the particular experiment.)

When applying the time-step analysis to the simulation data, we observed that V_g could be underestimated if there were time steps during which the length of a MT remained close to zero but displayed a small positive increase in length. We therefore imposed a "nucleation" threshold and counted a displacement only if the length of the MT above the seed was greater than or equal to the threshold for the entire time step (varying nucleation thresholds shown in **Figure S10A-B**). Note, this is not the same as imposing a threshold on the size of the displacement itself (as was done in the drift coefficient measurements in (Mauro et al., 2019)). In the V_g measurements here (**Figure 7** (square symbols), **Figure S10**), whenever the MT length was above the nucleation threshold, all positive displacements ($s_i > 0$) were counted.

Additionally, the value of V_g from the time-step analysis depends on the size of the time step (**Figure S10C-D**). If the time step is too small, the results will be affected by the velocity of upward fluctuations that are small and rapid, and the method will therefore overestimate the actual velocity of the extended growth phases of DI. If the time step is too large, there will be individual displacements that include some shortening (despite being net positive), and the method will therefore underestimate V_g. Our results indicate that time steps within an intermediate range produce similar results to each other (e.g., time steps ~2-5 seconds in simplified model and ~1-5 seconds in detailed model; **Figure S10C-D**).

The time-step method could also be used to estimate V_s by restricting to only negative displacements. However, accurate measurement of V_s may require using a smaller time step than accurate measurement of V_g, because shortening phases tend to have faster velocities and last for shorter amounts of time than growth phases (see also (Mauro et al., 2019)).

Automated quantitative analysis of dynamic instability

For the analyses in **Figures 5C-D** (+ symbols), **7** (+ symbols), **9** (+ symbols), **S5A** (all symbols), and **S8B,D,F,H** (+ symbols), it is necessary to identify periods of growth and shortening in length history data and to measure the DI parameters (V_g = growth velocity during growth phases, V_s = shortening velocity during shortening phases, F_{cat} = frequency of catastrophe, and F_{res} = frequency of rescue). To obtain these measurements, we developed an automated MATLAB

program (code available upon request). This automated program was applied here to simulated data, but can be applied to any length history data.

Overview of the DI analysis method: The analysis program uses the MATLAB function 'findpeaks' to identify major peaks in the length history data with a user-defined threshold for peak prominence (**Figure S11A,C**). The peak prominence is the height of the peak relative to the valley that is nearest to the peak, without a larger intervening peak (the nearest valley can be either before or after the peak). The ascent to each major peak is classified as a growth phase, and the descent from each major peak is classified as a shortening phase. The point of the transition from growth to shortening at a major peak (**Figure S11A,C**) is identified as a catastrophe (**Figure S11B,D**). A transition from shortening to growth at a major valley (**Figure S11A,C**) is considered to be a rescue (**Figure S11B)** *only if* the MT length at the transition is greater than or equal to a user-defined threshold.

The DI parameters are calculated as follows, where the totals are over all detected phases (of growth or shortening, as indicated) for all individuals in the population:
V_g = (total length change during growth phases) / (total time spent in growth phases),
V_s = (total length change during shortening phases) / (total time spent in shortening phases),
F_{cat} = (total number of catastrophes) / (total time spent in growth phases),
F_{res} = (total number of rescues) / (total time spent in shortening phases).

Finding major peaks, major valleys, and minor valleys: The first step in the analysis uses the MATLAB function 'findpeaks' to identify major peaks in the length history data that have a peak prominence of at least 25 subunit lengths (200 nm) (**Figure S11A,C**). Next, the function 'findpeaks' is applied to the negative of the length data to identify *major* valleys, with prominence of at least 25 subunit lengths, and *minor* valleys, with prominence of at least 0.5 subunit lengths. (In the detailed model, the outputted MT length is the average of the lengths of the 13 protofilaments, so the MT length can have non-integer values).

Determining the start and end points of each growth/shortening segment: At a catastrophe event (**Figure S11B,D**), the end of the growth phase and the start of the shortening phase are chosen to be the same point in time as each other (at a major peak, **Figure S11A,C**). Similarly, at a rescue event (**Figure S11B**), the end of shortening and the start of growth are identified as occurring at the same time point (at a major valley, **Figure S11A**, if the major valley is above the rescue threshold of 25 subunit lengths). However, if the MT length at a major valley is below the rescue threshold (as in **Figure S11C**), then the start of the growth phase may be at a later time than the end of the preceding shortening phase (**Figure S11D**, zoom-in in **Figure S11E**). In this case, the procedure described in the legend of **Figure S11** is used to choose the points to be identified as the end of the shortening phase and the start of the growth phase.